

# Helicases DDX5 and DDX17 promote heterogeneity in HBV transcription termination in infected human hepatocytes

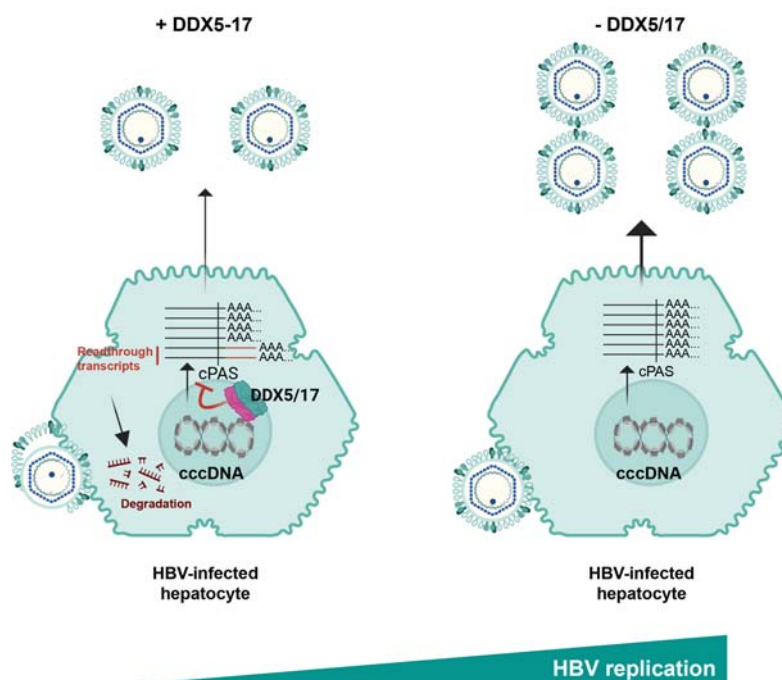
## Authors

Fleur Chapus, Guillaume Giraud, P lagie Huchon, ..., Cyril F. Bourgeois, Fabien Zoulim, Barbara Testoni

## Correspondence

barbara.testoni@inserm.fr (B. Testoni), fabien.zoulim@inserm.fr (F. Zoulim).

## Graphical abstract



## Highlights

- We uncovered a heterogeneous transcriptional termination of HBV transcripts in cellular models and in patients with CHB.
- HBV transcription termination is functionally linked to HBV replication.
- RNA helicases DDX5 and DDX17 promote HBV transcriptional read-through and viral RNA destabilisation.
- DDX5 and DDX17 are host HBV restriction factors and are downregulated in patients with CHB.

## Impact and implications

HBV covalently closed circular (ccc)DNA degradation or functional inactivation remains the holy grail for the achievement of HBV cure. Transcriptional fidelity is a cornerstone in the regulation of gene expression. Here, we demonstrate that two helicases, DDX5 and DDX17, inhibit recognition of the HBV polyadenylation signal and thereby transcriptional termination, thus decreasing HBV RNA stability and acting as restriction factors for efficient cccDNA transcription and viral replication. The observation that DDX5 and DDX17 are downregulated in patients chronically infected with HBV suggests a role for these helicases in HBV persistence *in vivo*. These results open new perspectives for researchers aiming at identifying new targets to neutralise cccDNA transcription.

# Helicases DDX5 and DDX17 promote heterogeneity in HBV transcription termination in infected human hepatocytes

Fleur Chapus<sup>1,2,†</sup>, Guillaume Giraud<sup>1,8,†</sup>, Pélagie Huchon<sup>1,2,8</sup>, Mélanie Rodà<sup>1,8</sup>, Xavier Grand<sup>1,8</sup>, Caroline Charre<sup>1,2,6</sup>, Chloé Goldsmith<sup>2</sup>, Armando Andres Roca Suarez<sup>1,8</sup>, Maria-Guadalupe Martinez<sup>1,2</sup>, Judith Fresquet<sup>1</sup>, Audrey Diederichs<sup>1,2,8</sup>, Maëlle Locatelli<sup>1,2</sup>, Hélène Polvèche<sup>4,5</sup>, Caroline Scholtès<sup>1,2,6,8</sup>, Isabelle Chemin<sup>1,8</sup>, Hector Hernandez Vargas<sup>2</sup>, Michel Rivoire<sup>7,8</sup>, Cyril F. Bourgeois<sup>5</sup>, Fabien Zoulim<sup>1,2,3,8,\*</sup>, Barbara Testoni<sup>1,8,\*</sup>

Journal of Hepatology 2024. vol. 81 | 609–620



**Background & Aims:** Transcription termination fine-tunes gene expression and contributes to the specification of RNA function in eukaryotic cells. Transcription termination of HBV is subject to the recognition of the canonical polyadenylation signal (cPAS) common to all viral transcripts. However, the regulation of this cPAS and its impact on viral gene expression and replication is currently unknown.

**Methods:** To unravel the regulation of HBV transcript termination, we implemented a 3' RACE (rapid amplification of cDNA ends)-PCR assay coupled to single molecule sequencing both in *in vitro*-infected hepatocytes and in chronically infected patients.

**Results:** The detection of a previously unidentified transcriptional readthrough indicated that the cPAS was not systematically recognized during HBV replication *in vitro* and *in vivo*. Gene expression downregulation experiments demonstrated a role for the RNA helicases DDX5 and DDX17 in promoting viral transcriptional readthrough, which was, in turn, associated with HBV RNA destabilization and decreased HBx protein expression. RNA and chromatin immunoprecipitation, together with mutation of the cPAS sequence, suggested a direct role of DDX5 and DDX17 in functionally linking cPAS recognition to transcriptional readthrough, HBV RNA stability and replication.

**Conclusions:** Our findings identify DDX5 and DDX17 as crucial determinants of HBV transcriptional fidelity and as host restriction factors for HBV replication.

© 2024 The Authors. Published by Elsevier B.V. on behalf of European Association for the Study of the Liver. This is an open access article under the CC BY-NC-ND license (<http://creativecommons.org/licenses/by-nc-nd/4.0/>).

## Introduction

Despite treatments that can efficiently control infection, HBV cannot be fully eradicated from infected hepatocytes.<sup>1</sup> Viral persistence is due to the so-called covalently closed circular DNA (cccDNA) that acts as a viral minichromosome in the nucleus of infected hepatocytes. cccDNA is the unique template for the transcription of the six main viral mRNAs by the host RNA polymerase II (RNAP II), including the pregenomic RNA (pgRNA). The latter is then retro-transcribed and encapsidated to generate new infectious particles. Thus, silencing transcriptional activity of cccDNA is considered a promising therapeutic approach to achieve a functional cure of chronic HBV infection.<sup>2</sup>

Similarly to host transcripts, HBV RNAs are subjected to a series of co-transcriptional processing events that not only contribute to their maturation, but also regulate HBV replication and contribute to HBV-induced liver diseases.<sup>3</sup> Co-transcriptional HBV RNA polyadenylation is initiated by the

recognition of a polyadenylation signal (cPAS) common to all HBV transcripts as a termination signal for the RNAP II. Its sequence, UAUAAA, is derived from the consensus mammalian PAS sequence AAUAAA.<sup>4</sup> Furthermore, *in vitro* assays showed that both 5' and 3' PAS-surrounding sequences are critical for its proper recognition and thus for a proper 3' end processing of HBV transcripts.<sup>4,5</sup> However, the molecular mechanisms governing proper transcription termination and how it influences HBV replication remain open questions.

RNA helicases play fundamental roles in the regulation of gene expression, including transcription termination and 3' end mRNA processing.<sup>6</sup> Members of this protein family appeared to act as enhancers or repressors of HBV replication.<sup>7</sup> Among these proteins, the highly redundant ATP-dependent RNA helicases DDX5 and DDX17 were shown to couple transcription and co-transcriptional mRNA processing to fine-tune gene expression during differentiation processes.<sup>6,8</sup> In particular,

\* Corresponding authors. Address: INSERM U1052- Cancer Research Center of Lyon (CRCL), 69008 Lyon, France.

E-mail addresses: [barbara.testoni@inserm.fr](mailto:barbara.testoni@inserm.fr) (B. Testoni), [fabien.zoulim@inserm.fr](mailto:fabien.zoulim@inserm.fr) (F. Zoulim).

† These authors contributed equally as first authors

‡ These authors contributed equally as senior authors

<https://doi.org/10.1016/j.jhep.2024.05.016>



DDX5 and DDX17 act as regulators of transcription termination and 3' end mRNA processing in several cellular models.<sup>9–11</sup> DDX5 has also been identified as an HBV restriction factor contributing to silencing of the transcriptional activity of cccDNA,<sup>12</sup> while the role of DDX17 in the HBV lifecycle remains controversial.<sup>13,14</sup> Notably, these previous studies were performed in the transformed hepatoma cell lines HepG2-NTCP.

Here, in addition to HepG2-NTCP cells, we used non-transformed primary human hepatocytes (PHHs), as well as patient liver tissue samples, and combined 3' rapid amplification of cDNA ends (RACE)-PCR and single molecule sequencing using the Oxford Nanopore Technology (ONT) MinION to accurately map the 3' extremity of HBV transcripts *in vitro* and *in vivo*. We demonstrated that, while most HBV RNAs end 14 nucleotides downstream of the HBV cPAS, a proportion of viral transcripts display a transcriptional readthrough spanning around 700 nucleotides. Inhibition of this readthrough following DDX5/17 silencing identified DDX5 and DDX17 as critical regulators of HBV cPAS recognition. Furthermore, we demonstrated that this transcriptional readthrough promoted by DDX5 and DDX17 was associated with HBV RNA destabilization. Accordingly, we provide evidence that DDX5/17 knockdown and, consequently, the preferential usage of the HBV cPAS were associated with enhanced HBV replication, establishing a functional link between transcriptional termination and proper viral replication.

## Materials and methods

### Ethics statement

PHH were isolated from surgical liver resections after informed consent of patients (IRB agreements #DC-2008-99 and DC-2008-101).

The protocol for the use of liver samples from two patients with chronic hepatitis B (CHB) was approved by the competent Institutional Ethics Committee (CPP Sud est IV 11/040, authorization number DC-2008-235). Written informed consent was obtained from all patients and/or their legal guardians prior to liver biopsy.

### Additional materials and methods

All experimental procedures and materials are available in the supplementary information.

### Statistical analysis

Data are expressed as mean  $\pm$  SEM. Non parametric Mann-Whitney or Kruskal-Wallis tests were performed using Graph-Pad Prism 9 to evaluate the statistical significance. Two-tailed *p*-value was calculated for a risk threshold = 0.05.

## Results

### Mapping of 3' extremity of HBV transcripts reveals differential recognition of polyadenylation signal

We used HepG2-NTCP cells and PHHs, two validated cellular models to study HBV replication, to characterize the 3' extremity of viral transcripts 8 days post-infection, when viral replication is well established.<sup>15–17</sup> We set-up an HBV-specific 3'RACE approach coupled to PCR that, given the overlapping

nature of HBV RNAs, allows the amplification of the 3' end of all viral transcripts. If the cPAS was systematically used for viral transcript termination, the size of the generated amplicon would be  $\sim$ 500 bp in length (Fig. 1A).<sup>4</sup> Agarose gel electrophoresis in both cellular models confirmed the specificity of the approach and revealed a major, but smeary, band of the expected size, suggesting some degree of heterogeneity in the length of the 3' region of HBV transcripts (Fig. S1A).

Sequencing profiles obtained by single molecule ONT MinION analysis of 3' RACE amplicons revealed that the majority of reads had a size of  $\sim$ 500 bp, but a significant proportion of reads reaching up to  $\sim$ 1,100 bp was also observed, confirming the existence of heterogeneity in the length of the 3' end of HBV RNAs (Fig. 1A and S1B).

To better characterize these longer reads, a consensus sequence of 1,194 bp was generated by *de novo* assembly of the totality of the sequencing reads. The generated consensus was consistent across biological replicates and showed 98% identity with HBV genotype D genome by BLAST analysis (Fig. S1C). We then aligned every single sequencing read to this reference and visualized them using Integrated Genomics Viewer<sup>18</sup> (Fig. 1B). We observed an evident coverage drop at the position 463, *i.e.* 14 nucleotides downstream of the previously described cPAS<sup>4</sup> in both HepG2-NTCP cells and PHHs (Fig. 1B and S1D), reflecting a termination of the majority of reads at this position. This observation allowed us to locate the main HBV RNA termination site 14 nucleotides downstream of the cPAS, which is similar to eukaryotic cell transcripts that are cleaved between 10 and 30 nucleotides downstream of the PAS.<sup>19</sup> These data are in agreement with the main use of this cPAS as a termination signal for RNAP II and concordant with previous *in vitro* work.<sup>4</sup> Sequencing analysis confirmed that the longer reads shown in Fig. 1A correspond to single HBV transcripts extending up to 705 bp downstream of the cPAS in both cellular models (Fig. 1B and S1D), indicating a transcriptional readthrough. We looked for the consensus PAS sequence, NNTANA, obtained from the 12 mostly used PAS in the human genome, to determine whether potential alternative PAS (aPAS) could be used to terminate the transcription of these longer transcripts<sup>20</sup> (Fig. S1E). Besides the known cPAS (at the position 1,923 of the HBV genome) and the upstream aPAS1 (position 1,800),<sup>21</sup> several other consensus PAS sequences were bioinformatically identified in the transcriptional readthrough sequence, including the aPAS2 located 19 nucleotides upstream of the major end of the longer transcripts (at position 2,603 of the HBV genome), suggesting that aPAS2 could potentially be recognized as a termination signal (Fig. 1B and S1D,E).

Similar analyses performed in liver biopsies derived from two patients with CHB confirmed the results obtained in cellular models, with a major peak of reads of 450 bp corresponding to HBV transcripts ending 14 nucleotides downstream of the HBV cPAS (Fig. 1C,D, and S1F) and longer reads of different sizes going up to 705 bp downstream of the HBV cPAS (Fig. 1C,D).

Altogether, our data showed that HBV transcripts end 14 nucleotides downstream of the previously described HBV cPAS, but also pointed to the existence of a transcriptional readthrough terminating downstream of a putative aPAS, demonstrating that the viral cPAS is not systematically recognized as the unique termination signal for RNAP II.

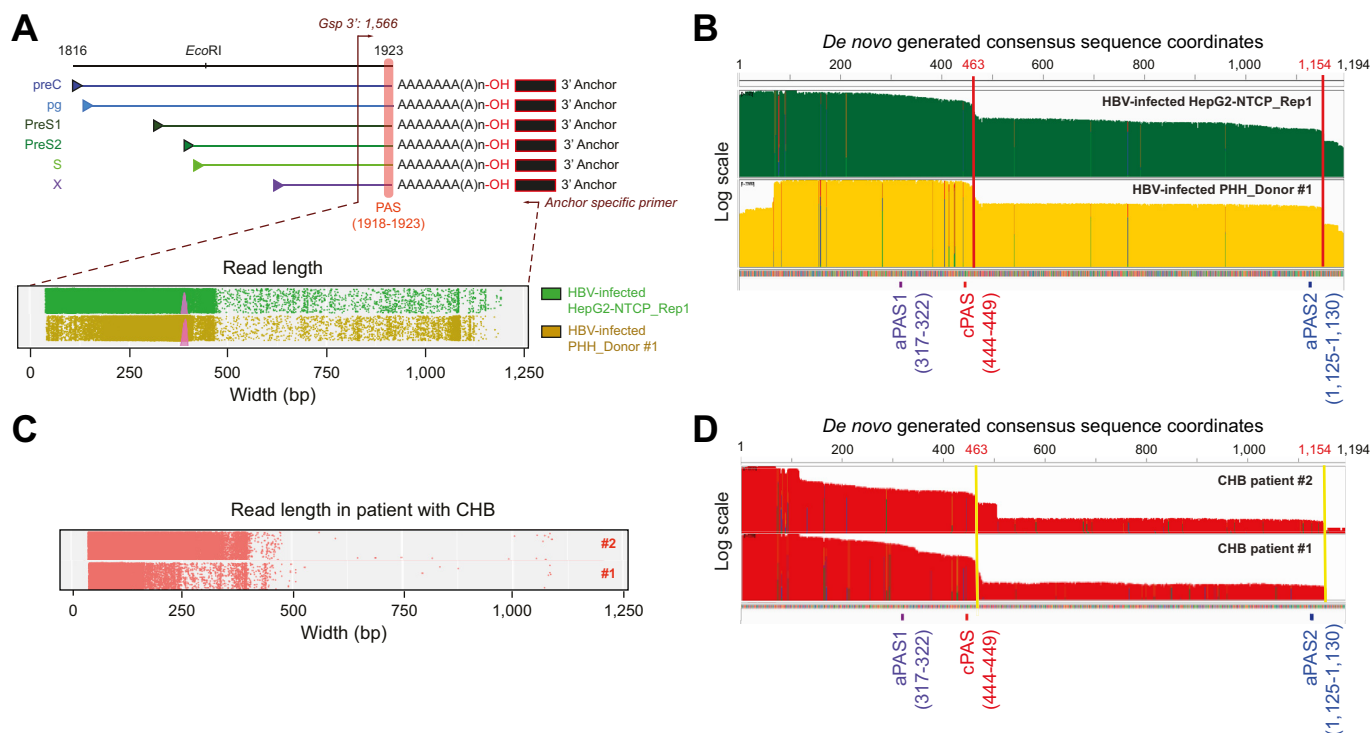


**Fig. 1. HBV transcripts end 14 nucleotides downstream of the cPAS and display transcriptional readthrough.** RNAs extracted from HepG2-NTCP cells and PHHs infected with HBV at MOI 250 for 8 days (A,B) and liver resections from two patients with CHB (C,D) were subjected to HBV-specific 3'RACE-PCR experiments followed by MinION single molecule sequencing. (A,C) Graphical representation of the read length obtained from the MinION single molecule sequencing of 3'RACE-PCR amplicons. Each dot corresponds to a single read. (B,D) IGV view of the Nanopore sequencing reads aligned to a *de novo* assembly-generated HBV consensus sequence. At the bottom, the position of PAS predicted by the Poly(A) Signal Miner prediction tool is indicated. The PAS indicated in red (cPAS) corresponds to the previously identified PAS known to be shared by every HBV transcript.<sup>4</sup> The vertical lines (red or yellow) correspond to the end of HBV transcripts. The scale used is a logarithmic scale. aPAS, alternative PAS; CHB, chronic hepatitis B; cPAS, canonical PAS; IGV, Integrated Genome Viewer; MOI, multiplicity of infection; PAS, polyadenylation signal; PHHs, primary human hepatocytes; RACE, rapid amplification of cDNA ends. (This figure appears in color on the web.)

### DDX5 and DDX17 favour the HBV transcriptional readthrough

The uncovering of HBV transcriptional readthrough led us to investigate the mechanisms regulating HBV cPAS recognition. Transcription termination and 3' end mRNA processing are tightly linked and regulated at both the chromatin and RNA level.<sup>22</sup> The ATP-dependent RNA helicases DDX5 and DDX17 play major roles in coupling transcription and co-transcriptional mRNA processing and were identified as constituents of protein complexes containing termination factors.<sup>8,9</sup>

Given the potential redundant functions of the helicases,<sup>8</sup> we concomitantly silenced both DDX5 and DDX17 in HBV-infected HepG2-NTCP cells 8 days post-infection (Fig. S2A,B) to test their potential role in HBV transcript termination. 3'RACE-PCR followed by agarose gel electrophoresis revealed several bands in the control RNAi condition (Fig. S2C), while a major band of around 500 bp was detected in DDX5/17-silenced HBV-infected HepG2-NTCP cells, suggesting a loss of heterogeneity in the 3' region of HBV transcripts when DDX5 and DDX17 were downregulated (Fig. S2C). ONT MinION single molecule sequencing of 3'RACE amplicons revealed that HBV-infected HepG2-NTCP cells transfected with non-targeting small-interfering RNA displayed the same pattern as non-transfected cells, with reads reaching up to around 1,200 bp

(Fig. 2A and S2D). Interestingly, these reads appeared to be significantly less frequent in DDX5/17-depleted HepG2-NTCP cells compared to control cells (Fig. 2A,B and S2D,E). We then aligned every read to the previously *de novo*-generated HBV reference genome and confirmed that the depletion of DDX5 and DDX17 decreased the frequency of transcriptional readthrough in favour of a termination 14 nucleotides downstream of the cPAS (Fig. 2C and S2F).

Similar experiments were performed in HBV-infected PHHs derived from two different donors (Fig. 2D–F and S2G–I). As observed in the HepG2-NTCP model, HBV transcripts displayed a reproducibly less frequent transcriptional readthrough in DDX5/17-depleted cells compared to control PHHs (Fig. 2D–F and S2G–I), confirming that DDX5 and DDX17 also prevented the recognition of the HBV cPAS in infected primary cells.

A potential redundant effect involving DDX5 and DDX17 in the regulation of HBV transcription termination was supported by the observation that silencing of either helicase triggered an increase in protein levels of the other one (Fig. S3A). Consistently, the 3' end phenotype of HBV RNAs showed no differences from the small-interfering control condition where the helicases were individually downregulated (Fig. S3B–D).

Altogether, these data showed that DDX5 and DDX17 are involved in HBV mRNA 3' end processing by preventing the

## Characterizing HBV transcription termination

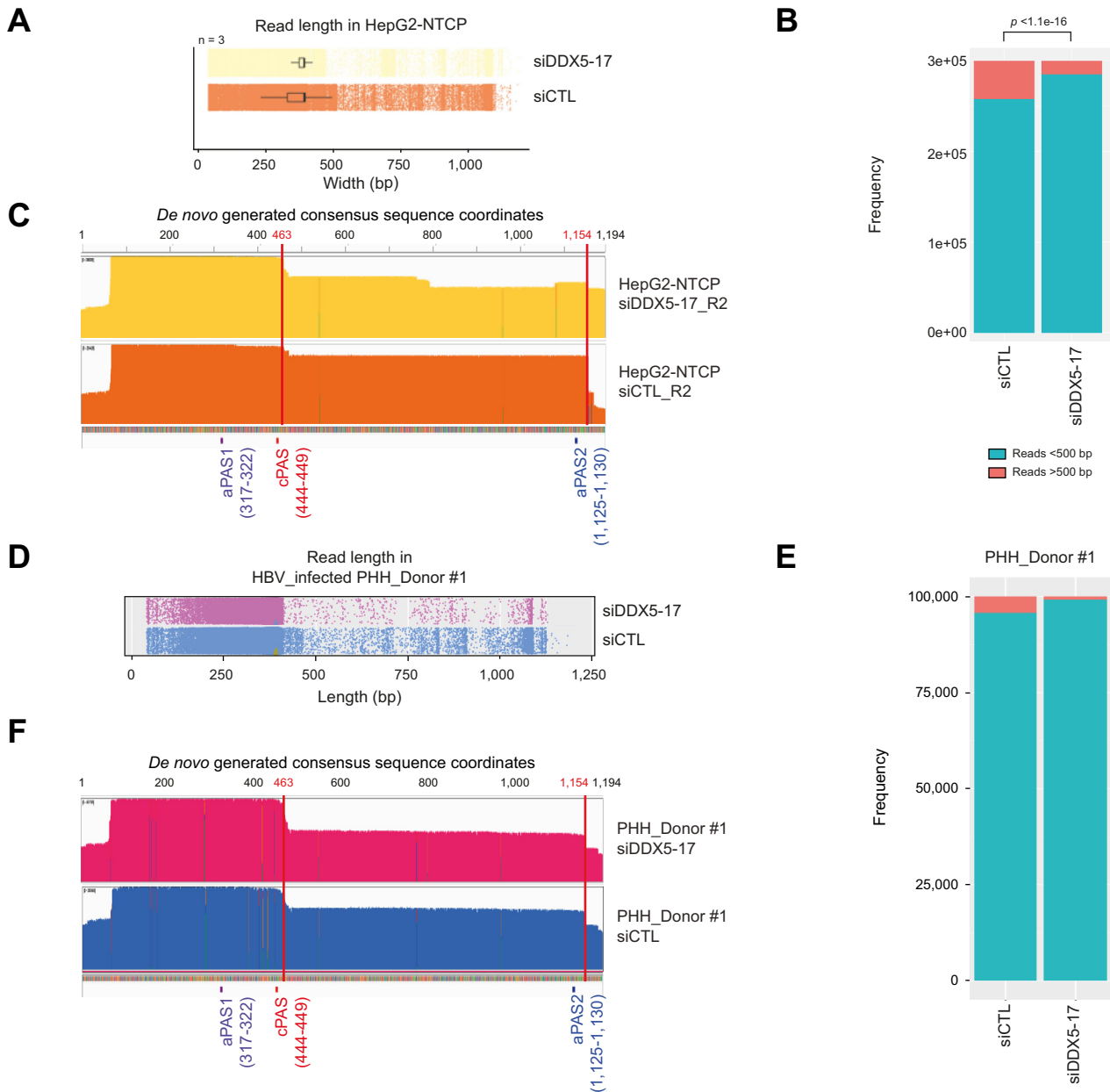


**Fig. 2. DDX5 and DDX17 favour the transcriptional readthrough.** HepG2-NTCP cells and PHHs were infected with HBV at MOI 250 for 8 days. (A,D) Graphical representation of the read length obtained from three independent MinION sequencing experiments of the 3'RACE-PCR amplicons obtained from HBV-infected HepG2-NTCP cells (A) or PHHs (D) transfected with control siRNA (siCTL) or DDX5/17-targeted siRNAs (siDDX5-17). Each dot corresponds to a single read. (B, E) Barplot indicating the frequency of the reads longer (in red) or shorter (in blue) than 500 bp obtained from the single molecule sequencing of the 3'RACE amplicons shown in Fig. S2C and S2I, respectively. Fisher test comparing the proportion of long to short reads,  $\alpha$  threshold = 0.05. (C,F) IGView of the MinION reads aligned to the *de novo* assembly generated HBV consensus reference genome and obtained from the HBV-infected HepG2-NTCP cells (C) or PHHs (F) transfected with control siRNA (siCTL) or with DDX5/17-targeted siRNA. MOI, multiplicity of infection; IGView, Integrated Genome Viewer; MOI, multiplicity of infection; PHHs, primary human hepatocytes; RACE, rapid amplification of cDNA ends; siRNA, small-interfering RNA. (This figure appears in color on the web.)

recognition of the cPAS and promoting HBV transcriptional readthrough.

### DDX5 and DDX17 are not involved in the first passage of the cPAS during 3.5 kb RNA transcription

The cPAS must remain unrecognized when RNAP II first encounters it during the transcription of 3.5 kb RNAs.<sup>23</sup> To test if silencing of DDX5-17 could have an impact on this event, we

employed two strategies based on the use of an engineered replication competent HBV 1.3 plasmid.<sup>24</sup> In this construct, the region between nucleotide 823 and 1990, which contains the cPAS, is duplicated at both the 5' end and the 3' end of the construct (Fig. S4A). This conformation implies that the cPAS located at the 5' end must not be recognized for the expression of pgRNA to take place.

The first strategy consisted of inserting an EGFP coding sequence in frame with the HBc ATG containing a STOP codon

located at position 1906, upstream of the cPAS position in the 5' redundant region (Fig. S4A). This means that EGFP expression will not be affected by the recognition of the first cPAS. We also inserted an mCherry coding sequence in frame with the POL ATG, whose expression, on the contrary, is prevented by the termination of RNAP II at the 5' cPAS. Therefore, the mCherry/EGFP ratio will be modified if DDX5 and DDX17 regulate the recognition of the 5' cPAS. We thus performed reverse-transcription quantitative PCR (RT-qPCR) experiments from HepG2-NTCP cells (silenced or not for both DDX5 and DDX17 and transfected with this modified HBV 1.3 construct, Fig. S4B) and compared the ratio of mCherry/EGFP mRNA expression. The results showed no difference between control and silenced cells (Fig. S4C).

The second strategy consisted of inserting two point mutations upstream of the 5' cPAS while the corresponding nucleotides in the 3' region remained unmodified (Fig. S4D). If DDX5 and DDX17 regulate the first passage of the cPAS, the proportion of transcripts containing the mutated nucleotides would be increased compared to the wild-type (WT). Again, we performed silencing of DDX5-17 in HepG2-NTCP cells transfected with this modified 1.3 construct (Fig. S4E). After RT-PCR using primers surrounding the single nucleotide polymorphisms and amplifying both the 5' and 3' mutated region of the construct, we sequenced the amplicons and analysed the electropherogram using EditR software<sup>25</sup> (Fig. S4F). This tool measures the efficiency of Cas9-mediated editing on the target sequence. In line with the results obtained with the first strategy, no difference in the proportion of mutated vs. WT amplicons was found between control and silenced cells (Fig. S4G). Taken together, these data suggest that DDX5 and DDX17 do not regulate the first cPAS passage during the synthesis of the 3.5 kb RNAs.

Altogether, these data argue against a role for DDX5 and DDX17 in the recognition of the 5' cPAS by RNAP II during the transcription of 3.5 kb RNAs.

### DDX5 and DDX17 bind cccDNA and HBV RNAs

To determine whether DDX5 and DDX17 act directly to promote HBV transcriptional readthrough, we first analysed the transcriptome of HBV-infected HepG2-NTCP cells depleted or not for both RNA helicases by RNA-seq experiments. DESeq2 gene expression analysis identified 1,585 upregulated and 2,088 downregulated genes after the repression of DDX5 and DDX17 ( $\log_2$ foldchange > |1|). Gene ontology analyses performed using GenePattern website (<https://www.genepattern.org>) did not identify terms related to 3' end mRNA processing or transcription termination, suggesting that DDX5 and DDX17 do not regulate genes involved in this process in the experimental conditions analysed (Fig. 3A).

In parallel, we investigated the ability of both RNA helicases to bind cccDNA and HBV RNAs. Chromatin immunoprecipitation (ChIP)-qPCR (Fig. 3B) and UV-crosslinking immunoprecipitation (CLIP) RT-qPCR (Fig. 3C) were carried out in HBV-infected HepG2-NTCP cells. cccDNA and HBV RNAs showed a specific enrichment compared to negative controls (Ctrl IgG and  $\beta$ -globin locus for ChIP and H3.3 and No Ab for CLIP) when antibodies against either DDX5 or DDX17 were used for immunoprecipitation (Fig. 3B,C). These data demonstrate that DDX5 and DDX17 are recruited to HBV

cccDNA and RNAs and suggest that they could play a direct role in the recognition of cPAS and, thus, in the regulation of HBV 3' end mRNA processing.

### Lengthening of the 3'UTR destabilizes HBx transcripts

The transcriptional readthrough of HBV transcripts results in the lengthening of their 3' untranslated region (3'UTR). 3'UTR is a critical regulatory region for RNA metabolism and the site of recruitment of regulators such as RNA binding proteins or microRNAs, known to dictate RNA stability, export and/or translation.<sup>26</sup>

To unveil the impact of the transcriptional readthrough on HBV RNA metabolism, we focused on its effect on the HBx transcript, which codes for the HBx protein, indispensable for HBV infection.<sup>27</sup> To mimic the lack of cPAS recognition observed in the DDX5/17-depleted condition, we engineered expression vectors (pcDNA6) bearing the HBx coding sequence fused at its 5' end to a V5 tag coding sequence and at its 3' end to the 3'UTR region encoded by the transcriptional readthrough carrying a WT (cPASwt) or mutated cPAS (TATAAA to CGCGGG, cPASmut) (Fig. 4A).

After transfection of HepG2-NTCP cells (Fig. S5), the levels of total HBx transcripts and HBx transcripts bearing a long 3'UTR (long HBx) were quantified by RT-qPCR experiments. While the levels of total HBx transcripts produced by the cPASmut constructs did not appear to be significantly different from the cPASwt (Fig. 4B), the cPASmut construct produced a significantly higher proportion of long HBx transcripts than the cPASwt construct (Fig. 4C). Strikingly, long HBx transcripts produced by the cPASwt construct could still be detected, further confirming that the cPAS is not systematically recognized as a termination signal for RNAP II in this construct, similarly to the HBV genome after infection (Figs 1 and 4C).

We then tested the impact of the long 3'UTR on HBx transcript stability. We treated cPASwt- and cPASmut-transfected HepG2-NTCP cells with actinomycin D (ActD), a transcription inhibitor, for 9 h and quantified the remaining levels of total HBx transcripts by RT-qPCR. We observed a significantly faster degradation of total HBx transcripts produced by the cPASmut constructs compared to those produced by the cPASwt construct (Fig. 4D). Since we observe a significant increase of RNAs presenting a readthrough in the cPASmut condition, these data strongly suggest that the presence of a longer 3'UTR destabilizes HBx transcripts.

Finally, we compared HBx protein levels produced by cPASwt- and cPASmut-transfected HepG2-NTCP cells. Western blot analyses using an anti-V5 antibody revealed that the cPASmut construct produced significantly less HBx protein than the cPASwt construct (Fig. 4E), demonstrating the strong association of a longer 3'UTR with HBx RNA destabilization and lower HBx protein levels.

### DDX5 and DDX17 repress HBx by promoting transcriptional readthrough

To establish a functional link between DDX5-17 expression and the transcriptional readthrough, we tested the effect of DDX5 and DDX17 up- or downregulation on the HBx RNA and protein levels in cPASwt and cPASmut-transfected HepG2-NTCP cells (Fig. S6A,B). Silencing of DDX5 and DDX17 increased the

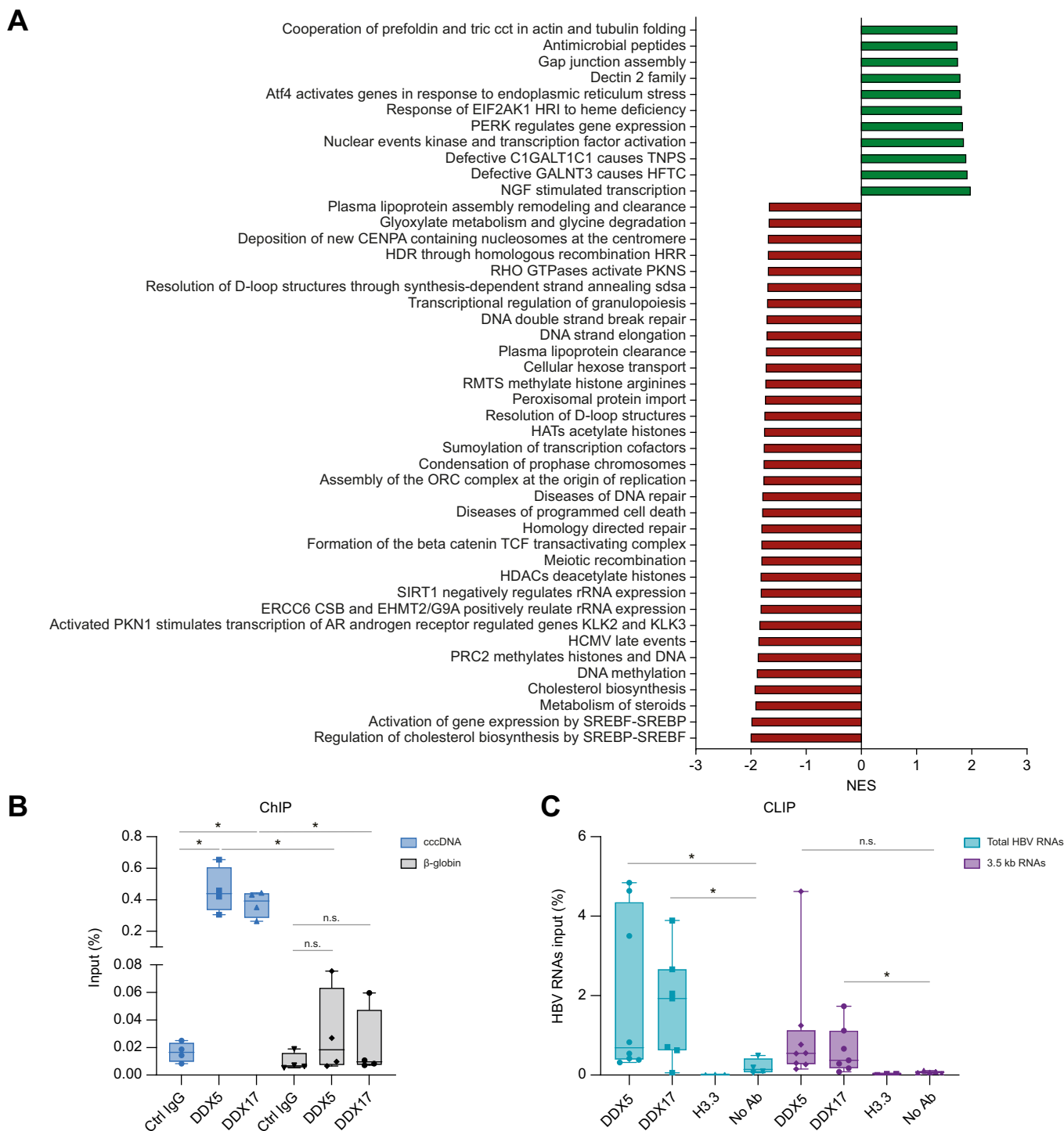


**Fig. 3. Direct role of DDX5 and DDX17 in the regulation of HBV transcription termination.** (A) Signalling pathways enriched from the list of upregulated (green bars) and downregulated (red bars) genes after DDX5 and DDX17 repression in HBV-infected HepG2-NTCP cells identified by RNA-Seq followed by gene ontology analyses using GenePattern. (B) ChIP experiments were performed from crosslinked HBV-infected HepG2-NTCP cells using an anti-DDX5, an anti-DDX17 or a control rabbit IgG (Ctrl IgG) followed by qPCR experiments to amplify precipitated cccDNA (blue boxes) or a β-globin negative control region (grey boxes). The graph represents the percentage of cccDNA or β-globin present in the input material. Each dot represents one biological replicate. Boxplots represent the average of the three (DDX5) or four (DDX17 and No Ab) independent biological replicates and the error bars represent the SEM. \*Mann-Whitney  $p < 0.05$ . (C) CLIP experiments were performed from UV-crosslinked HBV-infected HepG2-NTCP cells using an anti-DDX5, an anti-H3.3 antibody or without antibody (No Ab) followed by RT-qPCR experiments with assays detecting all HBV transcripts (total HBV RNAs, green) or 3.5 kb RNAs (purple). The graph represents the percentage of HBV RNAs present in the input material. Each dot represents one biological replicate. Boxplots represent the average of two (H3.3) or six (DDX5, DDX17 and No Ab) independent biological replicates and the error bars represent the SEM. \*Mann-Whitney  $p < 0.05$ . cccDNA, covalently closed circular DNA; CLIP, UV-crosslinking immunoprecipitation; RT-qPCR, reverse-transcription PCR. (This figure appears in color on the web.)

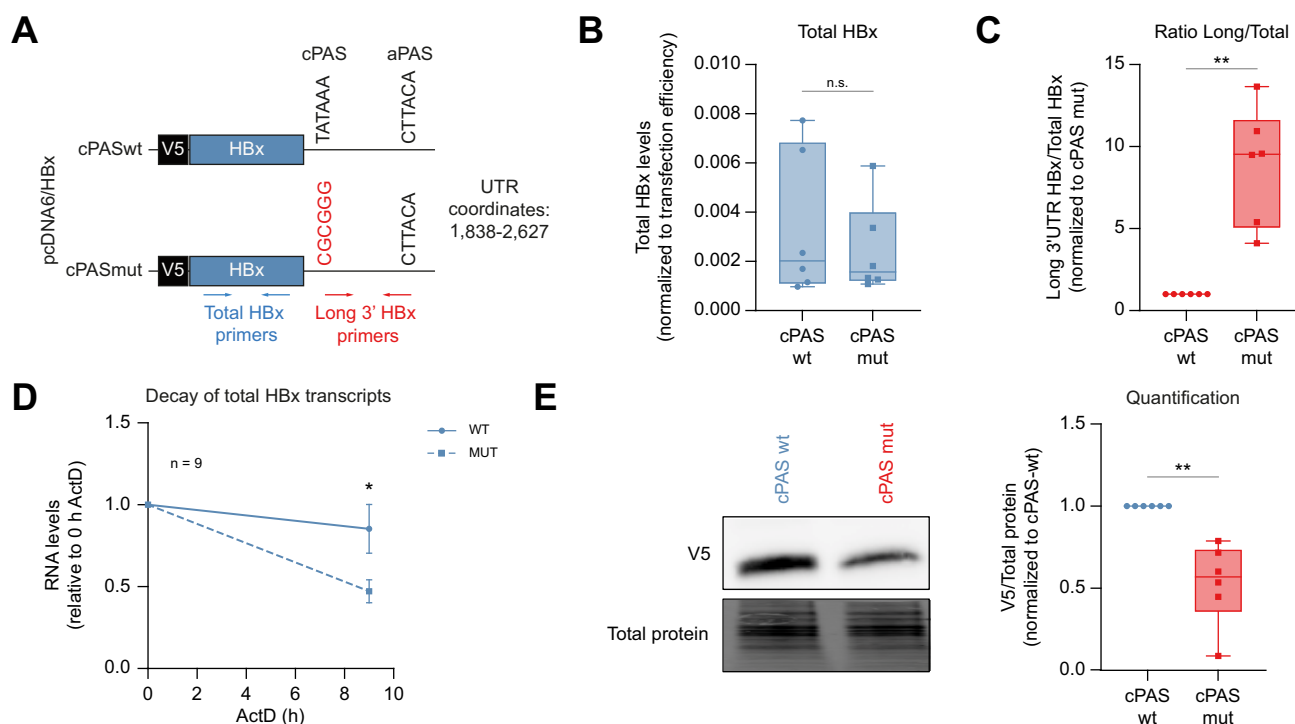


**Fig. 4. HBV transcriptional readthrough destabilizes HBx transcripts.** HepG2-NTCP cells were transfected with either the cPASwt or the cPASmut constructs (A). Two days after, RNAs and proteins were collected and analysed by RT-qPCR and Western blot, respectively. (B,C) Quantification of HBx transcripts with assays recognizing all forms (total, B) and only long (C) HBx RNAs by RT-qPCR. Levels of total HBx transcripts were normalized to the levels of *GAPDH* mRNAs and of transfected pcDNA6 plasmids quantified by qPCR (Fig. S3B). Levels of long HBx transcripts were normalized to the levels of total HBx transcripts. Each dot represents one biological replicate. Boxplots represent the first quartile, the median (horizontal line) and the third quartile of six independent biological replicates. Error bars represent the minimal and maximal values. (D) cPASwt (full lines) and cPASmut (dashed lines)-transfected HepG2-NTCP cells were treated with 20  $\mu$ g/ml ActD for 9 h. RNAs were extracted at 0 and 9 h post-treatment and subjected to RT-qPCR to amplify total HBx transcripts. Each time point represents the average  $\pm$  SEM of nine independent biological replicates. (E) Quantification of V5 protein levels by Western blot analyses using an anti-V5 antibody. Total proteins blots used as loading controls were obtained after activation of the stain-free gels. Boxplots represent the densitometry quantification of the V5 signal normalized to the corresponding signal for total proteins and expressed as fold change with respect to the cPASwt-transfected condition. n.s.: Mann-Whitney  $p > 0.05$ ; \*Mann-Whitney  $p < 0.05$ ; \*\*Mann-Whitney  $p < 0.01$ ; \*\*\*\*Mann-Whitney  $p < 0.0001$ . ActD, actinomycin D; RT-qPCR, reverse-transcription PCR. (This figure appears in color on the web.)

global level of total HBx transcripts produced by the two constructs, in accordance with a previously described role for DDX5 as an HBV transcriptional repressor<sup>12</sup> (Fig. 5A). However, the proportion of long HBx transcripts was decreased only when the cPASwt construct was transfected, whereas it was not affected by DDX5-17 silencing in the cPASmut condition (Fig. 5B). As previously observed (Fig. 4E), HBx protein levels were lower in the cPASmut condition compared to the cPASwt conditions (Fig. 5C). Strikingly, DDX5-17 silencing induced an increase of HBx protein levels produced from both constructs, thus reflecting the mixed effect of both the increase in total HBx transcripts and the decrease of the transcriptional readthrough (Fig. 5C). Overexpression of DDX5 and DDX17 either individually (Fig. S6C-E) or in combination (Fig. 5D-F) did not affect the levels of total HBx transcripts (Fig. 5D), but significantly increased the proportion of long HBx RNAs produced from the cPASwt construct but not from the cPASmut construct (Fig. 5E). This imbalanced proportion of longer HBx transcripts in the cPASwt condition was associated with decreased levels of HBx protein (Fig. 5F).

Altogether, these data strongly suggest that DDX5 and DDX17 repress HBx protein expression at least by promoting the transcriptional readthrough through a mechanism dependent on the recognition of the cPAS sequence.

#### DDX5 and DDX17 silencing stabilizes HBV RNAs in HBV-infected HepG2-NTCP cells and promotes viral replication

Then, we investigated if DDX5 and DDX17 were involved in the regulation of the stability of HBV RNAs produced in HBV-infected HepG2-NTCP cells. Indeed, treatment of HBV-infected HepG2-NTCP cells with ActD for 9 h revealed a significantly slower degradation of total HBV RNAs after knockdown of DDX5 and DDX17 compared to control cells (Fig. 6A, left panel). Surprisingly, the slower degradation was less pronounced for 3.5 kb RNAs and appeared not to be statistically significant (Fig. 6A, central panel). *GUSB* transcript half-life was not impacted by DDX5 and DDX17 silencing (Fig. 6A, right panel), indicating a specific effect of DDX5 and DDX17 silencing on HBV RNAs. 5'RACE-PCR experiments were carried out after ActD treatment to investigate the effect of DDX5-17 silencing on HBx transcript stability in the context of infection. Specific amplification of the canonical HBx transcript was ensured by the use of a junction primer between the 5'RACE anchor and the transcription start site of the canonical HBx transcript<sup>23</sup> (Fig. S7A,B). DDX5-17 silencing significantly increased HBx transcript stability, in line with our previous observations generated using the HBx-expressing plasmid (Figs 5 and 6B).



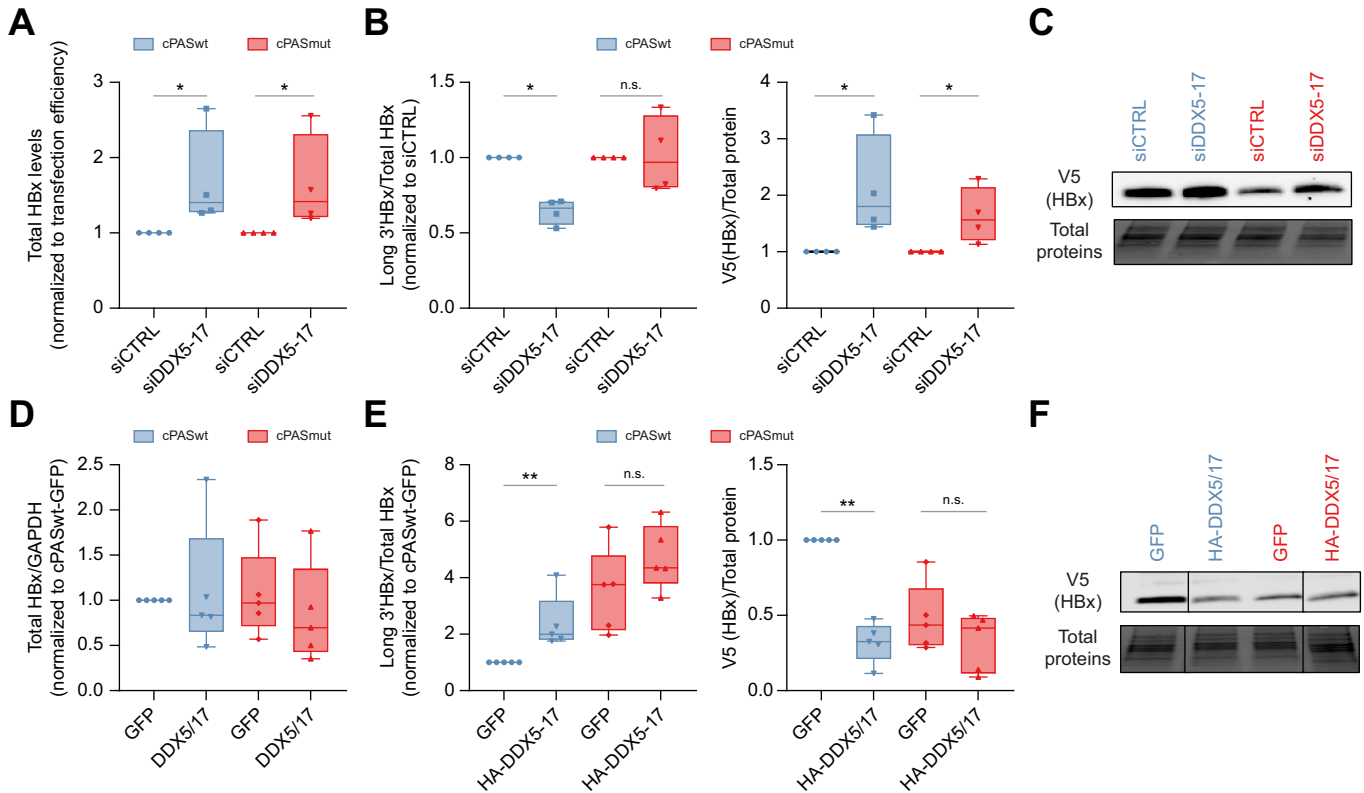


**Fig. 5. DDX5 and DDX17 regulate HBx expression by promoting transcriptional readthrough.** (A-C) HepG2-NTCP cells were transfected with control siRNAs (siCTRL) or siRNAs directed against *DDX5* and *DDX17* mRNAs one day prior to their transfection with either cPASwt or cPASmut constructs. Two days after the first transfection, RNAs and proteins were extracted and subjected to RT-qPCR (A,B) and western blot analyses (C) to quantify long HBx transcripts (A), total HBx transcripts (B) and HBx protein levels (C). (D-F) HepG2-NTCP cells were transfected with GFP or HA-DDX5 and HA-DDX17 expression plasmids one day prior to their transfection with either cPASwt or cPASmut constructs. Two days after the first transfection, RNAs and proteins were extracted and subjected to RT-qPCR (D,E) and western blot analyses (F) to quantify total HBx transcripts (D), long HBx transcripts (E) and HBx protein levels (F). (A,E) Long HBx transcript levels were normalized to total HBx transcript levels and the siCTRL-cPASwt (A) or the GFP-cPASwt (E) conditions. (B,D) Total HBx transcript levels were normalized to *GAPDH* levels and the siCTRL-cPASwt (B) or the GFP-cPASwt (D) conditions. (C,F) V5 (HBx) signal was quantified and normalized to the corresponding total protein load and siCTRL-cPASwt (C) or GFP-cPASwt (F) conditions. (A-E) Each dot represents one replicate. Boxplots represent the first quartile, the median (horizontal line) and the third quartile of four or five independent biological replicates. Error bars represent the minimal and maximal values. n.s.: Mann-Whitney  $p > 0.05$ ; \*Mann-Whitney  $p < 0.05$ . \*\*Mann-Whitney  $p < 0.01$ . RT-qPCR, reverse-transcription PCR; siRNA, small-interfering RNA. (This figure appears in color on the web.)

Accordingly, knockdown of *DDX5* and *DDX17* induced a significant increase of total HBV RNA levels (Fig. 6C and S7C,D). The levels of 3.5 kb RNAs were, instead, only slightly increased (Fig. 6C), prompting us to investigate if this was due to a higher rate of retrotranscription associated with the degradation of pgRNA mediated by the RNase H activity of the viral polymerase. To this end, we first quantified by qPCR the levels of cytoplasmic encapsidated HBV DNA after nucleocapsid isolation and showed that *DDX5* and *DDX17* silencing was associated with a significant increase of encapsidated HBV DNA levels in the cytoplasm of infected cells (Fig. 7A). In the same samples, NAGE (native agarose gel electrophoresis) coupled to western blotting analysis with anti-capsid (HBc) and envelope (HBs) HBV proteins revealed that the signal level of both cytoplasmic non-enveloped and enveloped capsids was also increased, thus showing enhanced virion formation and viral replication upon *DDX5/17* downregulation (Fig. 7B). This was accompanied by stable levels of cccDNA detected both by qPCR and Southern blotting (Fig. 7C and S10).

We then determined the effect of *DDX5-17* silencing on the stability of HBV transcripts generated from a capsid-null, encapsidation-deficient HBV 1.3 construct ( $\Delta$ HBc) (Fig. S8A).<sup>28</sup>

RT-qPCR experiments showed that while total HBV RNAs derived from both WT and  $\Delta$ HBc constructs were similarly increased in *DDX5-17*-silenced cells compared to control cells, only the 3.5 kb RNA levels produced from the  $\Delta$ HBc construct were significantly increased upon *DDX5-17* downregulation (Fig. S8B). Accordingly, ActD treatment confirmed that 3.5 kb RNAs were stabilized upon silencing of both helicases only in  $\Delta$ HBc-transfected cells (Fig. S8C), confirming that encapsidation and/or retrotranscription dynamics were responsible for the lack of detection of increased levels of 3.5 kb RNA species levels following *DDX5-17* silencing.

Altogether, these data establish a functional link between *DDX5* and *DDX17* expression, regulation of HBV transcription termination through the recognition of cPAS sequence, HBV RNA stability and viral replication.

#### **DDX5 and DDX17 expression is downregulated in hepatocytes from patients with CHB**

Our results highlight the role of *DDX5* and *DDX17* as HBV restriction factors. It was previously demonstrated that *DDX5* expression was inhibited in HBV-infected HepG2-NTCP cells

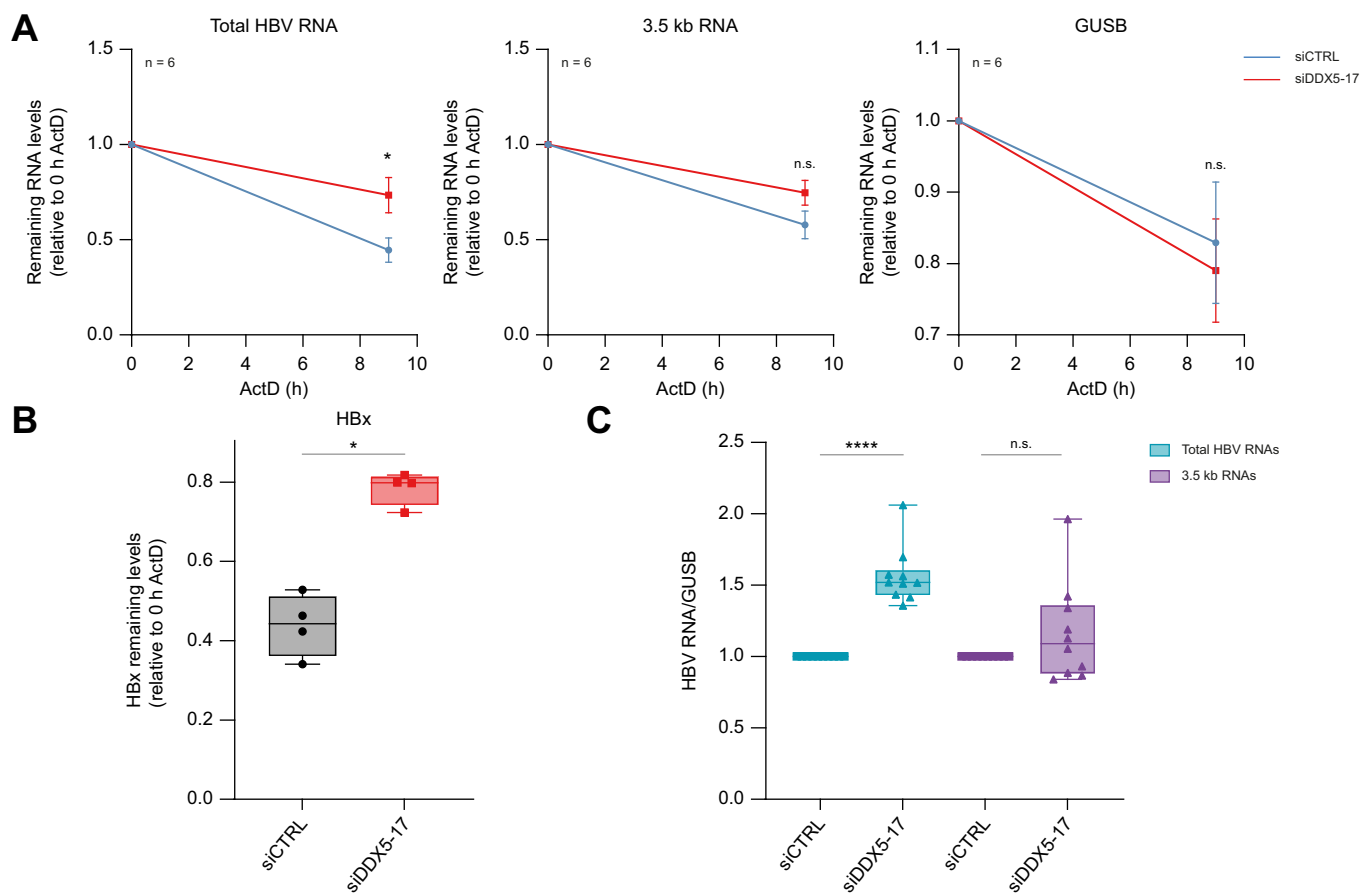


**Fig. 6. DDX5 and DDX17 repress and destabilize HBV RNAs.** HepG2-NTCP cells were infected at MOI 250 and transfected at 4 and 6 days post-infection with control siRNA (siCTRL) or siRNAs directed against *DDX5* and *DDX17* mRNAs (siDDX5-17). Eight days post-infection, RNAs were extracted and subjected to RT-qPCR analyses. (A,B) 20  $\mu$ g/ml ActD were added or not 9 h prior to RNA extraction. (A) The graphs represent the quantification of remaining levels of total HBV RNAs (left panel), 3.5 kb RNAs (center panel) or *GUSB* (right panel). Each time point represents the average of six independent biological replicates  $\pm$  SEM; (B) 5'RACE-PCR experiments were performed using a forward junction primer between the 5'RACE anchor and the canonical HBx TSS<sup>23</sup> and a reverse HBV-specific primer. Boxplots represent the first quartile, the median (horizontal line) and the third quartile of four independent biological replicates. Error bars represent the minimal and maximal values. (C) Quantification of total HBV RNAs (green) or 3.5 kb RNAs (purple). Levels of HBV RNAs were normalized to *GUSB* levels and expressed as fold change of the siCTRL condition. Boxplots represent the first quartile, the median (horizontal line) and the third quartile of ten independent biological replicates. Error bars represent the minimal and maximal values. n.s.: Mann-Whitney  $p > 0.05$ ; \*Mann-Whitney  $p < 0.05$ ; \*\*Mann-Whitney  $p < 0.01$ ; \*\*\*\*Mann-Whitney  $p < 0.0001$ . ActD, actinomycin D; MOI, multiplicity of infection; RACE, rapid amplification of cDNA ends; RT-qPCR, reverse-transcription PCR; siRNA, small-interfering RNA; TSS, transcription start site. (This figure appears in color on the web.)

and PHHs, as well as in a subset of HBV-related hepatocellular carcinoma.<sup>12</sup> Analysis of a single-cell RNA-Seq dataset derived from fine needle aspirates of 13 patients with CHB and three healthy donors (GSE234241<sup>29</sup>) allowed us to identify intrahepatic cell populations including hepatocytes (Fig. 8A and S9). Notably, *DDX5* and *DDX17* expression appeared to be down-regulated in hepatocytes from patients with CHB compared to healthy controls (Fig. 8B). These data support the idea that chronic HBV infection is associated with downregulation of helicases, which would contribute to lower frequency of HBV transcriptional readthrough and thus favour optimal viral replication and persistence of the virus *in vivo*.

## Discussion

Despite the identification of a PAS in the HBV genome decades ago,<sup>4</sup> the molecular mechanisms governing its recognition and its importance in HBV replication are still unresolved. Here, we characterized the 3' heterogeneity of HBV transcripts at the

single molecule level in *in vitro* cellular models, including PHHs, and in liver samples derived from patients with CHB. We found that the majority of HBV transcripts precisely stop 14 nucleotides downstream of the cPAS, confirming previous observations obtained from plasmid-derived HBs transcripts, which were shown to terminate between 12 and 19 nucleotides downstream of cPAS.<sup>4</sup> Interestingly, our results provide new information with the identification of previously overlooked HBV RNAs with a longer 3' region, extending approximately 700 bp after the cPAS, strongly suggesting the presence of a transcriptional readthrough. Using an HBx-expressing vector fused to this identified 3'UTR sequence, we demonstrated that readthrough transcription was associated with shorter RNA half-life and lower HBx protein expression. This observation was then confirmed for the authentic HBx transcript generated during HBV infection. Modulation of the size of 3'UTR region is known to serve as an additional mechanism of regulation of gene expression.<sup>26</sup> Most mechanisms proposed to explain this

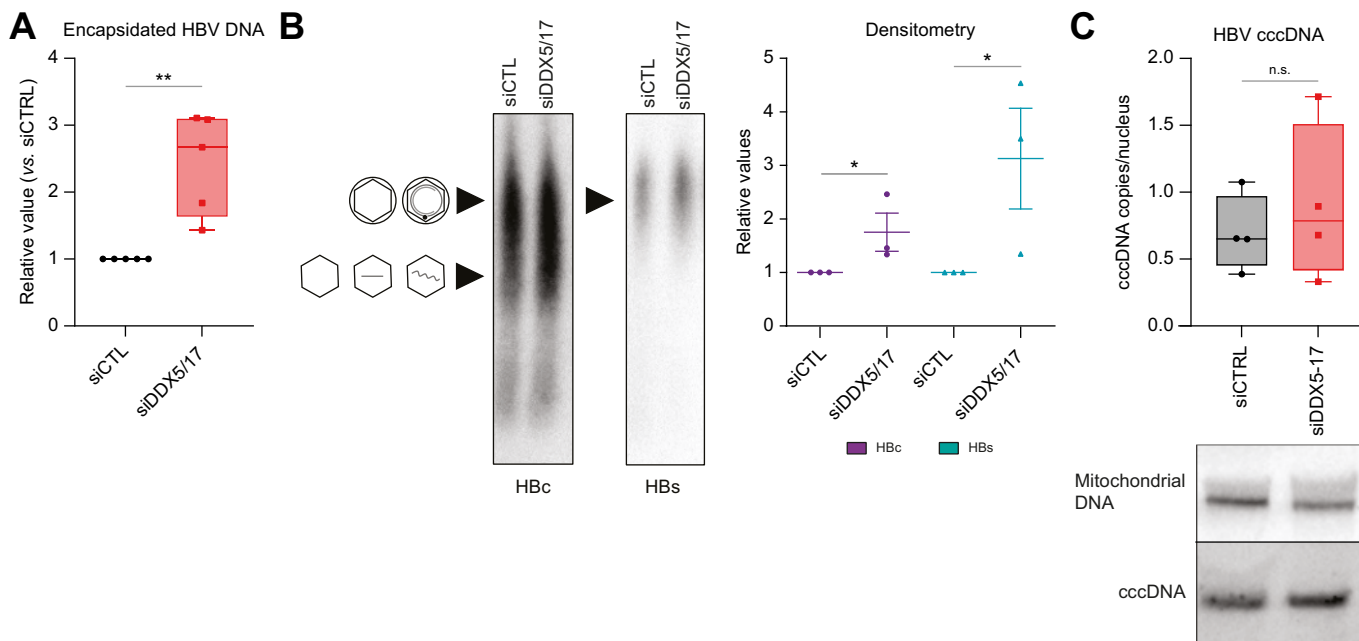


**Fig. 7. Repression of DDX5 and DDX17 increases HBV replication.** HepG2-NTCP cells were infected and transfected at 4 and 6 days post-infection with control siRNA (siCTRL) or siRNAs directed against *DDX5* and *DDX17* mRNAs (siDDX5-17). Samples were collected eight days post-infection. (A) HBV capsids obtained from the same number of cells in siCTRL and siDDX5/17 were isolated and HBV DNA isolated and quantified by qPCR. The data are expressed as fold change of the siCTRL condition. (B) NAGE of isolated viral particles in cell supernatant. *Left panel:* HBV particles were obtained from the same volume of lysate in each condition and detected by western blot using an HbC-specific antibody to detect capsids (rcDNA-containing and empty virions, upper, and naked capsids, lower) and an HBsAg-specific antibody to detect enveloped particles. *Right panel:* Boxplots represent the first quartile, the median (horizontal line) and the third quartile of the densitometry analysis of three independent experiments and data are expressed as fold change of siCTRL condition. Error bars represent the minimal and maximal values. n.s.: Mann-Whitney  $p > 0.05$ . \* $p < 0.05$  (Kruskal-Wallis multiple comparisons test); \*\*Mann-Whitney  $p < 0.01$ . (C) *Top panel:* DNA was isolated and digested with ExoI/ExoIII exonucleases and cccDNA was quantified by qPCR and normalized to the level of  $\beta$ -globin. *Bottom panel:* cccDNA and mitochondrial DNA (used as loading control) were visualized by Southern blot experiments using DIG-labelled specific probes against HBV DNAs. Uncut gel is presented in Fig. S5. cccDNA, covalently closed circular DNA; NAGE, native agarose gel electrophoresis; rcDNA, relaxed circular DNA; siRNA, small-interfering RNA. (This figure appears in color on the web.)

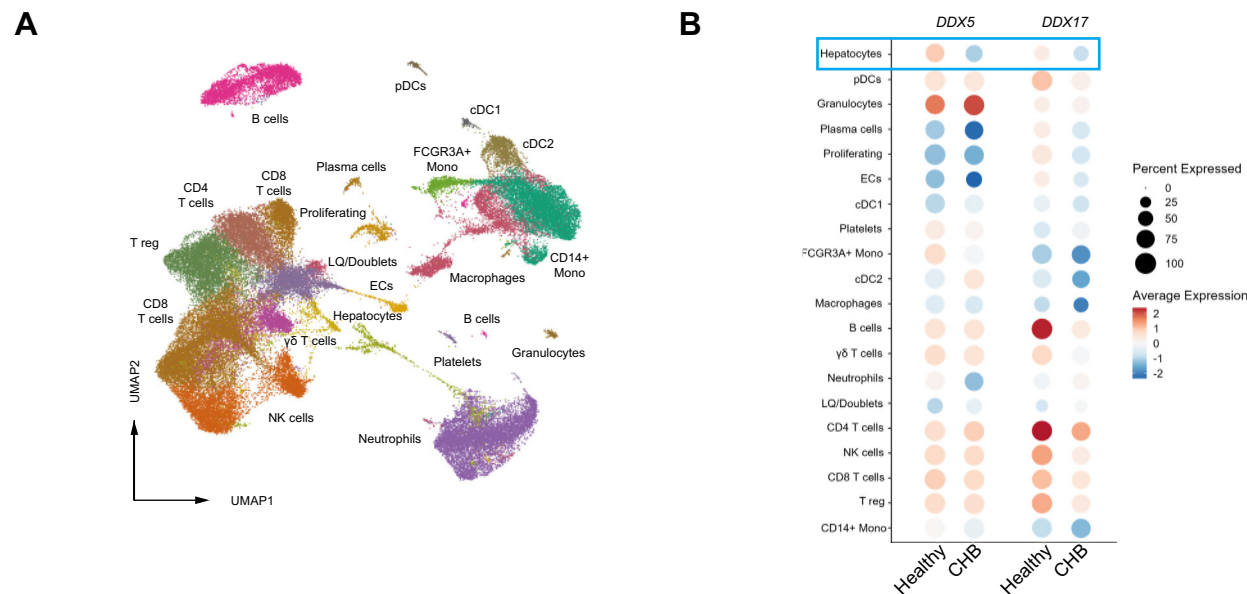


**Fig. 8. DDX5 and DDX17 expression are downregulated in hepatocytes of patients with CHB.** (A) UMAP plot of 20 hepatic cell populations identified following analysis of scRNA-seq data from patients with CHB ( $n = 13$ ) and healthy donors ( $n = 3$ ) (GSE234241). (B) Dotplot showing average expression levels and percentage of cells expressing *DDX5* and *DDX17* in each hepatic cell type according to viral status (GSE234241).<sup>29</sup> Hepatocytes are surrounded by a blue rectangle. cDCs, classical dendritic cells; CHB, chronic hepatitis B; FCGR3A, Fc gamma receptor IIIa; NK cells, natural killer cells; LQ, low quality; pDCs, plasmacytoid dendritic cells; UMAP, uniform manifold approximation and projection. (This figure appears in color on the web.)

regulation rely on the recruitment of trans-regulators of RNA metabolism.<sup>26</sup>

We identified DDX5 and DDX17 RNA helicases as critical promoters of HBV transcript readthrough. Their depletion strongly decreased readthrough transcription derived from natural HBV infection. The lack of effect on transcription termination when cPAS was mutated, together with the ChIP and CLIP data pointing at an association of the helicases with both HBV genome and RNAs, strongly suggest that DDX5/17 act via the regulation of cPAS recognition, although we cannot completely exclude an indirect contribution of other effectors regulated by DDX5 and DDX17. Our data also rule out a possible involvement of DDX5-17 in the non-recognition of the 5' cPAS by RNAP II during the transcription of 3.5 kb RNAs. This suggests that, most probably, sequences surrounding the cPAS in the nascent RNA are essential for its recognition as a PAS.<sup>4,5</sup>

The functional link we provided between DDX5/17-dependent HBV transcriptional fidelity and viral replication pointed at DDX5/17 as crucial restriction factors for HBV. Analysis of published single-cell RNA-Seq performed on liver fine needle aspirates derived from patients with CHB clearly highlighted a specific downregulation of *DDX5* and *DDX17* transcripts in HBV-infected hepatocytes *in vivo* (Fig. 8). Notably, it suggests that HBV would repress DDX5/17 expression *in vivo* to allow proper viral transcriptional fidelity and higher viral replication by decreasing the probability of having transcripts with longer 3'UTRs, which are less stable. It is therefore not surprising that these transcripts represent only a minority of the total HBV transcriptome in infected cells and in the analysed patients with CHB (Fig. 2). Moreover, given the crucial role of HBx in viral replication,<sup>27</sup> a precise termination of its transcript is thus necessary to ensure HBV infection establishment and persistence.

Both DDX5 and DDX17 were already identified as regulators of transcription termination.<sup>9–11</sup> However, their role in HBV seems to be the opposite to that in SHSY-5Y cells. The fact that the effect of DDX5/17 on transcription termination strongly depends on the chromatin topology of the regulated locus<sup>9</sup>

suggest a role for HBV minichromosome topology in their effect. Unfortunately, the small size of this episome has made it challenging to unravel its tri-dimensional conformation so far. In this respect, it would be interesting to investigate if DDX5-17 might play a role in the transcriptional fidelity of HBV-integrated sequences. However, the large majority of HBV integrations lack the cPAS and use either the upstream cryptic PAS or a host PAS.<sup>30</sup> Given that we do not see any difference in the usage of the HBV cryptic PAS upon DDX5-17 silencing in our experimental conditions, we might speculate that the helicases should not represent pivotal factors for HBV transcription termination of integrated sequences. However, it cannot be excluded that they could regulate the use of host PAS in HBV-host fusion transcripts.

Discordant results were obtained by different groups regarding the role of DDX5 or DDX17 in HBV replication. Indeed, DDX5 was shown to repress cccDNA transcription by stabilizing the PRC2 complex subunit SUZ12.<sup>12</sup> DDX17 was shown to inhibit pgRNA encapsidation by preventing the association between HBV polymerase and the pgRNA  $\varepsilon$ -motif in HepG2 cells.<sup>13</sup> However, Dong *et al.* recently showed opposite results, suggesting that HBx increased DDX17 expression, which, in turn, promoted HBV transcription and replication in HepG2-NTCP cells and in a hydrodynamic HBV mouse model.<sup>14</sup> Since DDX5 and DDX17 have redundant functions and cross-regulate themselves,<sup>8</sup> it cannot be excluded that these contrasting results might be due to the unbalanced ratio between the two helicases, a phenomenon we revealed after downregulating just one of them (Fig. S3). Here, the silencing of both DDX5 and DDX17 clearly demonstrated their joint role as HBV replication restriction factors.

Altogether, our data point out the pivotal importance of HBV transcription termination in HBV replication *in vivo* and provide a clear example of how co-transcriptional processing of HBV RNAs can modulate viral persistence. This study opens the door for a deeper understanding of the mechanisms controlling HBV transcription termination and their role in viral persistence and pathogenesis.

## Affiliations

<sup>1</sup>INSERM U1052, CNRS UMR-5286, Cancer Research Center of Lyon (CRCL), Lyon, France; <sup>2</sup>University of Lyon, UMR\_S1052, CRCL, 69008 Lyon, France; <sup>3</sup>Department of Hepatology, Hospices Civils de Lyon, France; <sup>4</sup>CECS/AFM, I-Stem, Corbeil-Essonnes, 91100, France; <sup>5</sup>University Claude Bernard of Lyon, Ecole Normale Supérieure de Lyon, CNRS UMR 5239, INSERM U1293, Laboratory of Biology and Modelling of the Cell, 69007, Lyon, France; <sup>6</sup>Department of Virology, Croix Rousse Hospital, Hospices Civils de Lyon, Lyon, France; <sup>7</sup>INSERM U1032, Centre Léon Bérard (CLB), 69008 Lyon, France; <sup>8</sup>The Lyon Hepatology Institute EVEREST, France

## Abbreviations

ActD, actinomycin D; aPAS, alternative PAS; cccDNA, covalently closed circular DNA; CHB, chronic hepatitis B; ChIP, chromatin immunoprecipitation; CLIP, UV-crosslinking immunoprecipitation; cPAS, canonical PAS; ONT, Oxford Nanopore Technology; PAS, polyadenylation signal; pgRNA, pregenomic RNA; PHHs, primary human hepatocytes; RACE, rapid amplification of cDNA ends; RNAP II, RNA polymerase II; RT-qPCR, reverse-transcription PCR; UTR, untranslated region; WT, wild-type.

## Financial support

This study was supported by a public grant attributed by the French Agence Nationale de la Recherche (ANR) as part of the second "Investissements d'Avenir" program (reference: ANR-17-RHUS-0003) to FZ and by "Investissement d'avenir" Laboratoires d'Excellence (LabEx) DEVweCAN (Cancer Development and Targeted

Therapies) grant ANR-10-LABX-61 to FZ and BT; by Agence Nationale de Recherches sur le SIDA, les Hépatites Virales et les Maladies Infectieuses Emergentes (ANRS MIE) grant ECTZ75178 to BT and CB and fellowship ECTZ161842 to GG.

## Conflict of interest

The authors declare no conflict of interest.

Please refer to the accompanying ICMJE disclosure forms for further details.

## Authors' contributions

Conceptualisation and formal analysis: FC, GG, BT. Funding acquisition: GG, BT, CFB, FZ. Investigation: FC, GG, PH, MR, MGM, AD, JF, ML. Methodology: GG, FC. Bioinformatics: XG, HP, CC, CG, AARS and CFB. Resources: CS, IC, FZ,

HHV, MR. Visualization: GG, FC, BT. Writing – original draft: GG, BT. Writing – review and editing: all authors.

### Data availability statement

The data presented in this manuscript are available through the corresponding author upon reasonable request.

### Acknowledgments

We would like to thank Maud Michelet, Jennifer Molle, Anaëlle Dubois and Sarah Heintz for their help in the isolation of primary human hepatocytes, as well as Prof. M. Rivoire's surgical staff for providing liver resections. We also would like to thank Emmanuel Combe for fruitful discussion regarding this study.

### Supplementary data

Supplementary data to this article can be found online at <https://doi.org/10.1016/j.jhep.2024.05.016>.

### References

*Author names in bold designate shared co-first authorship*

- [1] European Association for the Study of the Liver. EASL 2017 Clinical Practice Guidelines on the management of hepatitis B virus infection. *J Hepatol* 2017;67:370–398. <https://doi.org/10.1016/j.jhep.2017.03.021>.
- [2] Martinez MG, Boyd A, Combe E, et al. Covalently closed circular DNA: the ultimate therapeutic target for curing HBV infections. *J Hepatol* 2021;75:706–717. <https://doi.org/10.1016/j.jhep.2021.05.013>.
- [3] Chen A, Panjaworayan T, Thienprasert N, et al. Prospects for inhibiting the post-transcriptional regulation of gene expression in hepatitis B virus. *World J Gastroenterol* 2014;20:7993–8004. <https://doi.org/10.3748/wjg.v20.i25.7993>.
- [4] Simonsen CC, Levinson AD. Analysis of processing and polyadenylation signals of the hepatitis B virus surface antigen gene by using simian virus 40-hepatitis B virus chimeric plasmids. *Mol Cell Biol* 1983;3:2250–2258. <https://doi.org/10.1128/mcb.3.12.2250-2258.1983>.
- [5] Russnak RH. Regulation of polyadenylation in hepatitis B viruses: stimulation by the upstream activating signal PS1 is orientation-dependent, distance-independent, and additive. *Nucl Acids Res* 1991;19:6449–6456. <https://doi.org/10.1093/nar/19.23.6449>.
- [6] Bourgeois CF, Mortreux F, Auboeuf D. The multiple functions of RNA helicases as drivers and regulators of gene expression. *Nat Rev Mol Cell Biol* 2016;17:426–438. <https://doi.org/10.1038/nrm.2016.50>.
- [7] You H, Ma L, Wang X, et al. The emerging role of DEAD/H-box helicases in hepatitis B virus infection. *Front Cell Infect Microbiol* 2022;12.
- [8] Giraud G, Terrone S, Bourgeois CF. Functions of DEAD box RNA helicases DDX5 and DDX17 in chromatin organization and transcriptional regulation. *BMB Rep* 2018;51:613–622.
- [9] Terrone S, Valat J, Fontrodona N, et al. RNA helicase-dependent gene looping impacts messenger RNA processing. *Nucleic Acids Res* 2022;50:9226–9246. <https://doi.org/10.1093/nar/gkac717>.
- [10] Padmanabhan K, Robles MS, Westerling T, et al. Feedback regulation of transcriptional termination by the mammalian circadian clock PERIOD complex. *Science* 2012;337:599–602. <https://doi.org/10.1126/science.1221592>.
- [11] Katahira J, Ishikawa H, Tsujimura K, et al. Human THO coordinates transcription termination and subsequent transcript release from the HSP70 locus. *Genes Cells* 2019;24:272–283. <https://doi.org/10.1111/gtc.12672>.
- [12] Zhang H, Xing Z, Mani SKK, et al. RNA helicase DEAD box protein 5 regulates Polycomb repressive complex 2/Hox transcript antisense intergenic RNA function in hepatitis B virus infection and hepatocarcinogenesis. *Hepatology* 2016;64:1033–1048. <https://doi.org/10.1002/hep.28698>.
- [13] Mao R, Dong M, Shen Z, et al. RNA helicase DDX17 inhibits hepatitis B virus replication by blocking viral pregenomic RNA encapsidation. *J Virol* 2021;JV10044421. <https://doi.org/10.1128/JVI.00444-21>.
- [14] Dong M-L, Wen X, He X, et al. HBx mediated increase of DDX17 contributes to HBV-related hepatocellular carcinoma tumorigenesis. *Front Immunol* 2022;13:871558. <https://doi.org/10.3389/fimmu.2022.871558>.
- [15] Ko C, Chakraborty A, Chou W-M, et al. Hepatitis B virus genome recycling and de novo secondary infection events maintain stable cccDNA levels. *J Hepatol* 2018;69:1231–1241. <https://doi.org/10.1016/j.jhep.2018.08.012>.
- [16] Schulze-Bergkamen H, Untergasser A, Dax A, et al. Primary human hepatocytes—a valuable tool for investigation of apoptosis and hepatitis B virus infection. *J Hepatol* 2003;38:736–744. [https://doi.org/10.1016/s0168-8278\(03\)00120-x](https://doi.org/10.1016/s0168-8278(03)00120-x).
- [17] Yan H, Liu Y, Sui J, et al. NTCP opens the door for hepatitis B virus infection. *Antivir Res* 2015;121:24–30. <https://doi.org/10.1016/j.antiviral.2015.06.002>.
- [18] Thorvaldsdóttir H, Robinson JT, Mesirov JP. Integrative Genomics Viewer (IGV): high-performance genomics data visualization and exploration. *Brief Bioinform* 2013;14:178–192. <https://doi.org/10.1093/bib/bbs017>.
- [19] Zhao J, Hyman L, Moore C. Formation of mRNA 3' ends in eukaryotes: mechanism, regulation, and interrelationships with other steps in mRNA synthesis. *Microbiol Mol Biol Rev* 1999;63:405–445.
- [20] Beaudouin E, Freier S, Wyatt JR, et al. Patterns of variant polyadenylation signal usage in human genes. *Genome Res* 2000;10:1001–1010. <https://doi.org/10.1101/gr.10.7.1001>.
- [21] Kairat A, Beerheide W, Zhou G, et al. Truncated hepatitis B virus RNA in human hepatocellular carcinoma: its representation in patients with advancing age. *Intervirology* 1999;42:228–237. <https://doi.org/10.1159/000024982>.
- [22] Porrua O, Libri D. Transcription termination and the control of the transcriptome: why, where and how to stop. *Nat Rev Mol Cell Biol* 2015;16:190–202. <https://doi.org/10.1038/nrm3943>.
- [23] Stadelmayer B, Diederichs A, Chapus F, et al. Full-length 5'RACE identifies all major HBV transcripts in HBV-infected hepatocytes and patient serum. *J Hepatol* 2020;73:40–51. <https://doi.org/10.1016/j.jhep.2020.01.028>.
- [24] Ren S, Nassal M. Hepatitis B virus (HBV) virion and covalently closed circular DNA formation in primary Tupaia hepatocytes and human hepatoma cell lines upon HBV genome transduction with replication-defective adenovirus vectors. *J Virol* 2001;75:1104–1116. <https://doi.org/10.1128/JVI.75.3.1104-1116.2001>.
- [25] Kluesner MG, Nedveck DA, Lahr WS, et al. EditR: a method to quantify base editing from sanger sequencing. *CRISPR J* 2018;1:239–250. <https://doi.org/10.1089/crispr.2018.0014>.
- [26] Mayr C. What are 3' UTRs doing? *Cold Spring Harb Perspect Biol* 2019;11:a034728. <https://doi.org/10.1101/cshperspect.a034728>.
- [27] Slagle BL, Bouchard MJ. Role of HBx in hepatitis B virus persistence and its therapeutic implications. *Curr Opin Virol* 2018;30:32–38. <https://doi.org/10.1016/j.coviro.2018.01.007>.
- [28] Tu T, Zehnder B, Qu B, et al. De novo synthesis of hepatitis B virus nucleocapsids is dispensable for the maintenance and transcriptional regulation of cccDNA. *JHEP Rep* 2021;3:100195. <https://doi.org/10.1016/j.jhepr.2020.100195>.
- [29] Genshaft AS, Subudhi S, Keo A, et al. Single-cell RNA sequencing of liver fine-needle aspirates captures immune diversity in the blood and liver in chronic hepatitis B patients. *Hepatology* 2023;78:1525–1541. <https://doi.org/10.1097/HEP.000000000000438>.
- [30] Ramirez R, van Buuren N, Gamelin L, et al. Targeted long-read sequencing reveals comprehensive architecture, burden, and transcriptional signatures from hepatitis B virus-associated integrations and translocations in hepatocellular carcinoma cell lines. *J Virol* 2021;95. <https://doi.org/10.1128/jvi.00299-21>.

Keywords: RNA polyadenylation; transcription termination; RNA stability; RNA helicases; HBV.

Received 16 October 2023; received in revised form 28 March 2024; accepted 2 May 2024; available online 22 May 2024